Published in IET Microwaves, Antennas & Propagation
Received on 1st December 2013
Revised on 13th January 2014
Accepted on 11th February 2014
doi: 10.1049/iet-map.2013.0672

ISSN 1751-8725

Compact ultra-wideband diversity antenna with a floating parasitic digitated decoupling structure

Muhammad Saeed Khan[1], Antonio-Daniele Capobianco[1], Ali Imran Najam[2], Imran Shoaib[3], Elena Autizi[1], Muhammad Farhan Shafique[4]

[1]*Dipartimento di Ingegneria dell'Informazione, University of Padova, Via Gradenigo 6/b, 35131 Padova, Italy*
[2]*Laboratoire de Conception et d'Intégration des Systèmes (LCIS), Grenoble INP, 50 Rue Barthélémy de Laffemas BP-54, 26902 Valence Cedex 09, France*
[3]*School of Electronics Engineering and Computer Science, Queen Mary University of London, Mile End Road, London, UK*
[4]*Center for Advanced Studies in Telecommunication, COMSATS Institute of Information Technology, Park Road, Islamabad, Pakistan*
E-mail: khan@dei.unipd.it

Abstract: A compact planar ultra-wideband (UWB) multiple-input–multiple-output antenna array with two radiating elements is proposed in this work. Elements separation is kept at 5.5 mm and the isolation is achieved with a floating parasitic decoupling structure not known for UWB diversity antennas previously. The antenna system performs very well over the entire UWB frequency range of 3.1–10.6 GHz. The mutual coupling between the radiating elements is below −20 dB in most of the band. The decoupling structure is investigated in detail and the diversity analysis of the antenna in Rayleigh fading environment for indoor and outdoor propagations is also presented by computing envelope correlation coefficients. The proposed antenna array measures 33×45.5 mm^2 only and it is suitable for handheld devices, personal digital assistant (PDA)s, next generation home entertainment systems and robots.

1 Introduction

Ultra-wideband (UWB) frequency spectrum from 3.1 to 10.6 GHz is potential candidate for future wireless personal area networks (WPANs)-based communication devices. The power limitation of −41 dBm/MHz however creates a bottleneck in achieving the desired gigabit data link in a short range WPANs. The problem can be addressed by combining UWB and multiple-input–multiple-output (MIMO) techniques [1]. It increases the channel capacity and provides a reliable link by offering the benefits of MIMO technology without additional power requirements in a rich scattering environment [2, 3]. It is well established that the benefits of MIMO systems can be extended to its full potential by reducing the correlation among the propagating paths. The correlation not only depends on the propagation environment, but it is also strongly linked with the mutual coupling characteristics of the radiating antennas. Large coupling introduces signal leakage from one antenna to other, thus it not only increases the signal correlation but also reduces the radiation efficiency because of power dissipation at the coupled antenna's port.

Suppressing mutual coupling over a wideband is very challenging for diversity antennas; therefore various techniques like decoupling and matching networks, electromagnetic band-gap structures and neutralising line used in narrowband MIMO antennas are not applicable to UWB-MIMO antennas [4–7]. The focus thus remains on altering ground plane by employing defective ground structures (DGS) or by introducing stubs to enhance isolation over a wider bandwidth. In one of such studies, cone-shaped elements have been proposed with DGS, the bandwidth of the design is from 3.1 to 5.8 GHz with dimensions of 60×62 mm^2 [8]. Similarly, another design with 2×2 MIMO array employees DGS and covers frequency range from 2 to 6 GHz [9]. Stubs have been introduced in the ground plane in another work to achieve bandwidth from 2.27 to 10.2 GHz with dimensions of 64×60 mm^2 [10]. Similarly, another UWB diversity antenna has been proposed that uses stubs as decoupling elements and it covers bandwidth from 3.3 to 10.5 GHz with design dimensions of 45×62 mm^2 [11]. Recently a compact UWB diversity antenna has been introduced with tree like stubs in the ground plane to achieve impedance bandwidth from 3.1 to 10.6 GHz with isolation better than 16 dB [12]. It has been observed that the designs proposed earlier were either relatively large or they do not cover the complete UWB spectrum.

Parasitic elements are well known for enhancing gain in antennas [13–15]; however they have not been applied to enhance isolation between UWB diversity antenna elements. In this paper, a diversity antenna is proposed that employs a floating digitated parasitic element that provides a wideband isolation characteristics. The decoupling structure is introduced on the backside of diversity antenna and it provides coupling suppression of

better than 20 dB in most of UWB spectrum along with a very compact footprint.

2 Antenna structure

A standard circular monopole radiator was created with partial ground and it was later translated into a modified patch antenna with straight edges and arched feeding section through numerical simulations using commercially available simulator [16], in order to improve the impedance matching over wider bandwidth. The second radiator was then created on one side. Strong coupling was observed when they were in near proximity, so a floating parasitic digitated decoupling structure was introduced at the centre on the backside of the substrate. The decoupling structure is made of a horizontal conducting strip with vertical stubs of unequal lengths attached to it which are explained in Section 3. The antenna and decoupling structure design is shown in Fig. 1. The dotted line shows the original circular patch that was translated into the modified geometry.

The reflection coefficient and mutual coupling of antenna array with and without the decoupling structure is presented in Fig. 2.

The edge separation sp between the elements without decoupling structure was kept at 10 mm initially and it was later reduced to 5.5 mm when decoupling structure was introduced. It can be observed that the antennas couple strongly when they are brought closer to each other. A significant increase in mutual coupling can be observed when the edge separation was reduced from 10 to 5.5 mm. Later on when the decoupling structure was introduced, the isolation improved. The mutual coupling with decoupling structure at 5.5 mm separation is even lower than what it has offered at 10 mm separation without decoupling structure. Alongside, the return loss is also improved between 6 and 9 GHz band. The entire UWB range from 3.1 to 10.6 GHz is covered, reflection coefficient and mutual coupling is better than −10 and −20 dB, respectively, in most of the radiating band.

3 Working of digitated parasitic decoupling structure

The conventional concept of using stubs on the ground plane of radiator to achieve wideband performance has been extended to create parasitic elements on the backside of antenna. These strips are not connected to ground plane and they act as independent parasitic resonators. When these strips are arranged in the form of digits, the strips and slots formed in between them act as resonant elements for different frequencies and they help in improving isolation by adding multiple resonances in radiating band [12].

The resulting floating parasitic structure improves wideband characteristic of the proposed antenna array. The parasitic elements affect various antenna parameters as demonstrated for narrow band applications [13–15]. To elaborate the working of the decoupling structure, a full numerical parametric analysis was carried out. Different variations of decoupling structure were investigated (Fig. 3) and their effect on return loss and mutual coupling are shown in Figs 4 and 5, respectively. Initial simulation consists of only the main branch of decoupling structure and it introduced resonance at lower frequency around 4 GHz, later on branch 1 was added to the main branch (Fig. 3*b*).

By introducing the branch 1, isolation at lower frequencies increases and in the similar fashion adding branch 2 to the

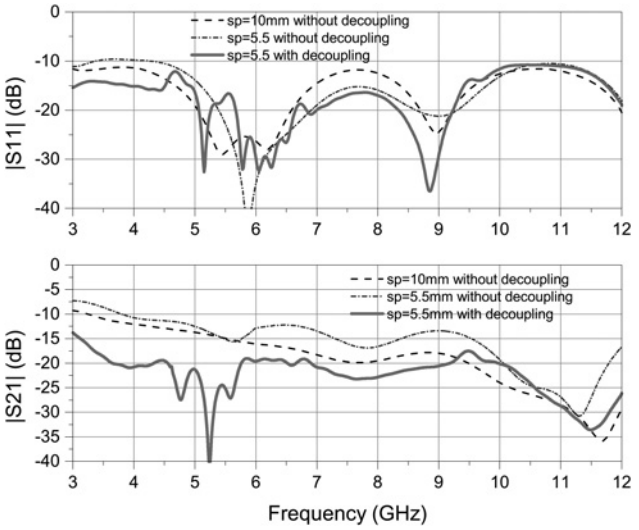

Fig. 2 *Simulated scattering-parameter of optimised UWB-MIMO antenna*

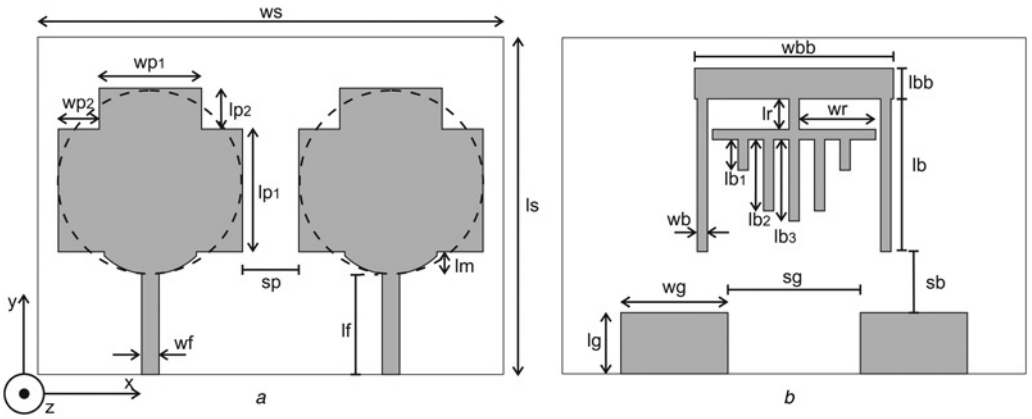

Fig. 1 *Geometry of the optimised antenna elements with decoupling structure*

a Top view
b Bottom view
Dimensions are $ws = 45.5$ mm, $ls = 33$ mm, $wp_1 = 10$ mm, $wp_2 = 4$ mm, $lp_1 = 12$ mm, $lp_2 = 4$ mm, $sp = 5.5$ mm, $lm = 2.1$ mm, $wf = 1.7$ mm, $lf = 9.9$ mm, $wg = 10.5$ mm, $lg = 6$ mm, $sg = 13$ mm, $wbb = 19.5$ mm, $lbb = 3$ mm, $wb = 1$ mm, $lb_1 = 3$ mm, $lb_2 = 7$ mm, $lb_3 = 8$ mm, $lr = 3$ mm, $wr = 7.5$ mm, $lb = 15$ mm and $sb = 6$ mm

doi: 10.1049/iet-map.2013.0672

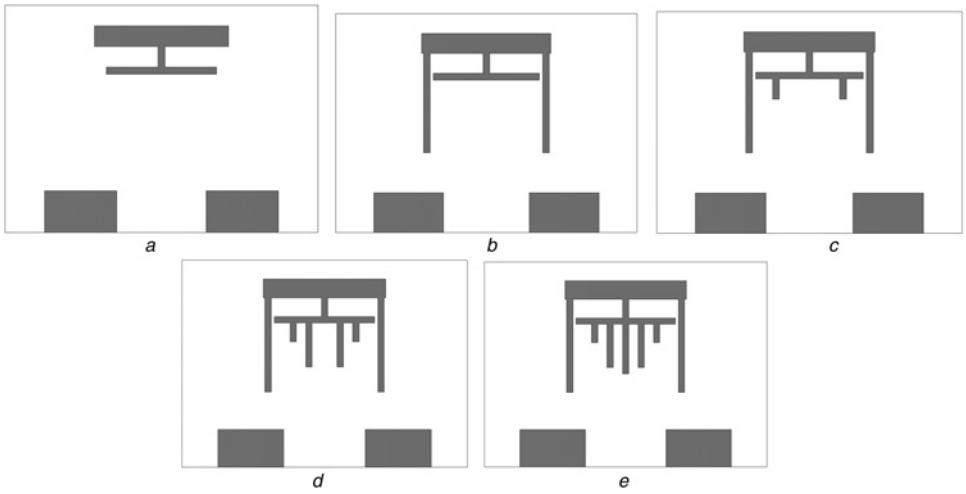

Fig. 3 *Different variations of decoupling structure*

a Main branch only
b Main branch and branch 1
c Main branch, branches 1 and 2
d Main branch, branches 1, 2 and 3
e Main branch, branches 1, 2, 3 and 4

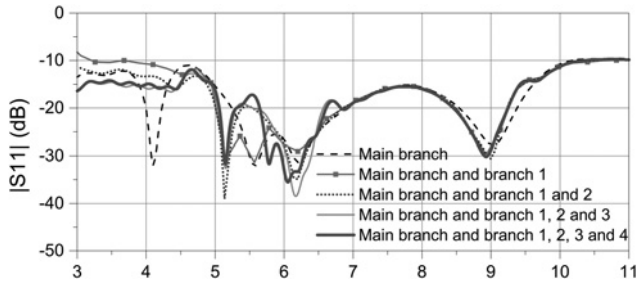

Fig. 4 *Effects of decoupling structure branches on |S11| parameter*

structure further improves the isolation at lower frequencies. Later on when branch 3 was added (Fig 3*d*), the isolation at middle UWB improves. Lastly, when all branches were added (Fig. 3*e*), the overall coupling suppression was observed, especially isolation improves at the higher frequencies. Decoupling structure acts as an isolator between the antenna elements. The digit count in the structure affects the isolation and bandwidth, large number of digits results in better isolation and wider bandwidth.

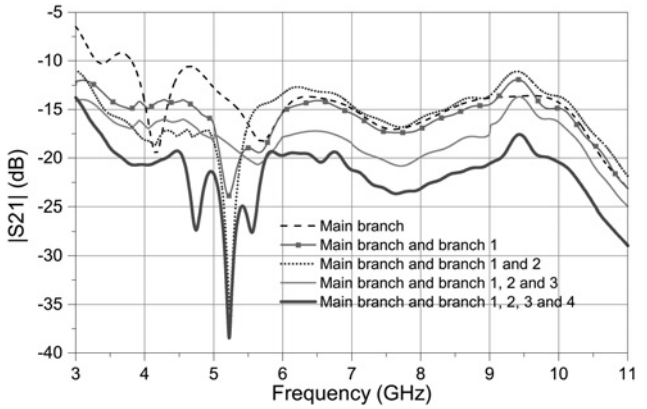

Fig. 5 *Effects of decoupling structure branches on |S21| parameter*

The mutual coupling is caused mainly by surface waves and space wave for closely placed antennas. The coupled radiation introduces current on the neighbouring antenna. The proposed decoupling structure captures the coupling fields and converts them in surface current hence reducing the mutual coupling. To investigate the effect of the decoupling structure, the surface current at 3.5, 7 and 10 GHz are shown in Fig. 6.

The surface current distribution indicates the influence of the decoupling structure. The induced current on the neighbouring antenna is reduced significantly when the decoupling structure is introduced. In all cases, the patch on the left was excited, whereas other element was terminated with a matched load. The induced current can be clearly seen on the decoupling element that reduces the current induction on the neighbouring antenna.

4 Fabrication and experimental results

The proposed design was fabricated on a Roger RO4003 laminate with a thickness of 1.524 mm, having dielectric constant of 3.55 and loss tangent of 0.0027. A photograph of the prototype is shown in Fig. 7.

4.1 Return loss and mutual coupling

The prototype was tested using Agilent N5242A PNA-X vector network analyser (VNA). A comparison of simulated and measured results is provided in Fig 8. A slight variation in the measured results is attributed to fabrication imperfection and lossy connectors. However, the overall measured results show return loss better than −10 dB in complete band and isolation better than 20 dB in most of the band except at lower UWB frequencies.

4.2 Radiation patterns, gain and efficiency

The radiation patterns of the proposed UWB diversity antenna were measured in an anechoic chamber at different frequencies. The measured and simulated radiation patterns at 3.5, 7 and 10 GHz are presented in Fig. 9.

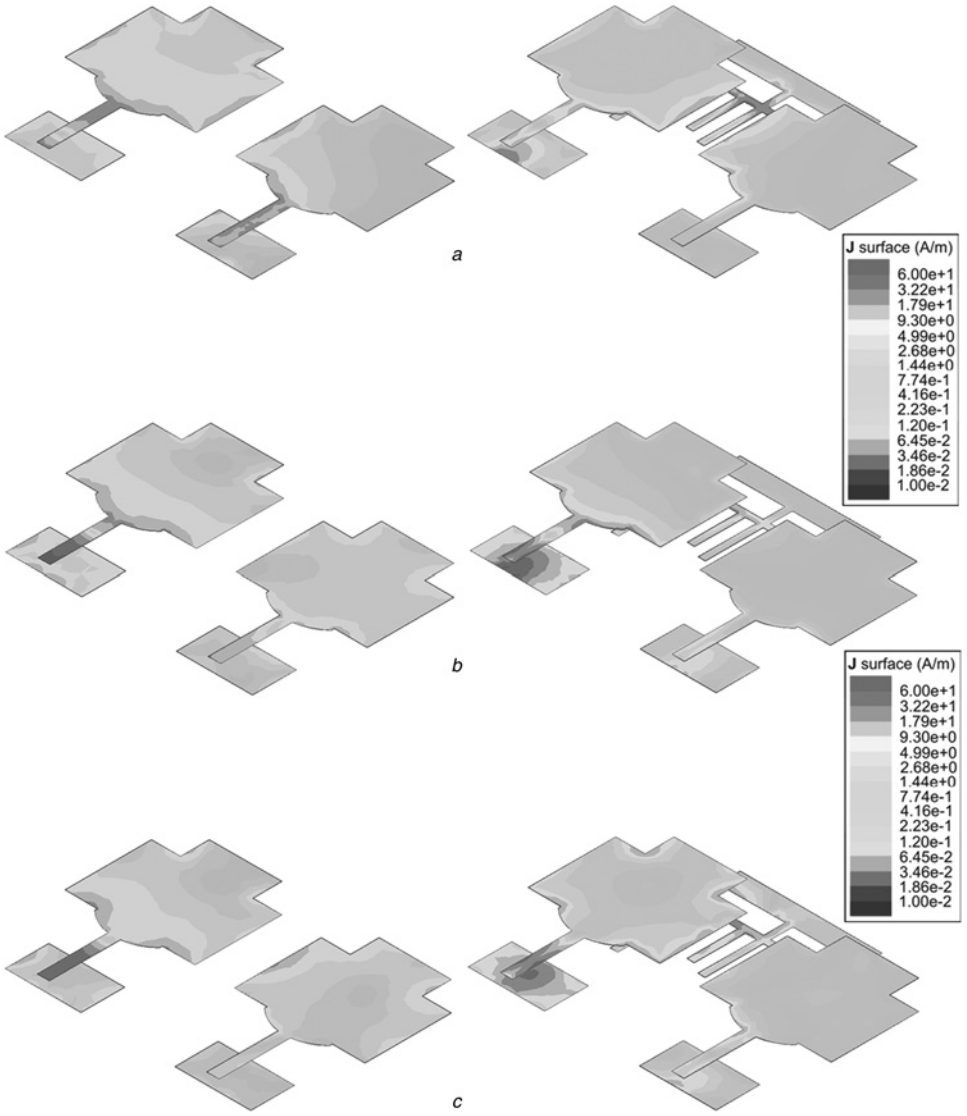

Fig. 6 *Surface current distribution without (left side) and with (right side) decoupling structure with left radiator excited at*
a 3.5 GHz
b 7 GHz
c 10 GHz

During the measurements one of the antennas was excited, whereas the other was terminated with a load of 50 Ω. *E* and *H* plane radiation patterns are in agreement with simulations at lower and middle UWB frequencies however at 10 GHz

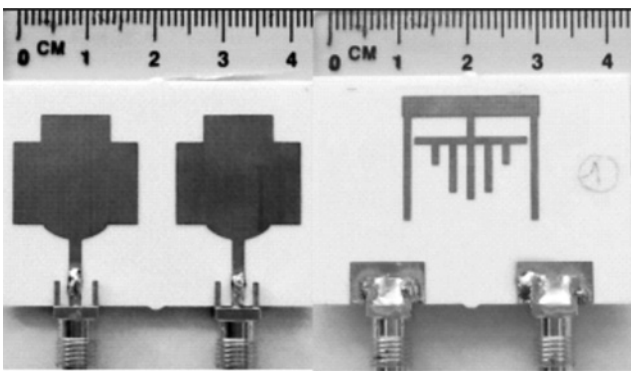

Fig. 7 *Photograph of fabricated prototype*

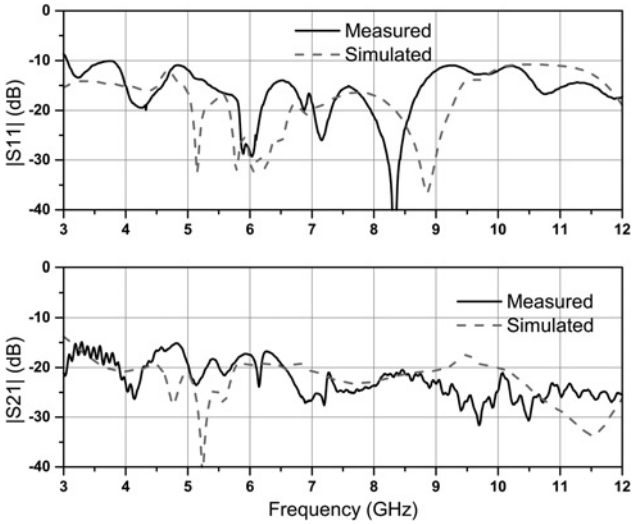

Fig. 8 *Simulated and measured scattering-parameters of the proposed antenna system*

doi: 10.1049/iet-map.2013.0672

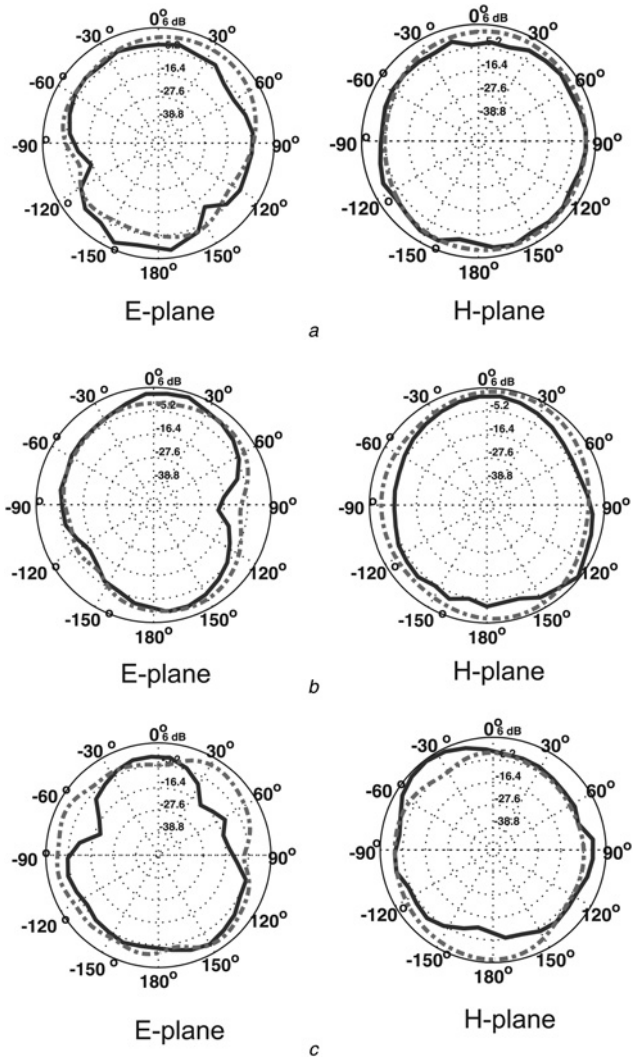

Fig. 9 *Simulated (dotted line) and measured (solid line) radiation patterns at*

a 3.5 GHz
b 7 GHz
c 10 GHz

and above the pattern shows distortion especially around 60° and −60°, the reason being measuring setup limitations, connector losses and possible reflection from second port because of unmatched termination. The antenna peak gain as a function of frequency is plotted in Fig. 10.

The gain variation without decoupling structure is 4 dBi, however, this variation reduces to <2.3 dBi with a peak gain of 5.3 dBi, when the decoupling structure is inserted, which makes it more consistent over the radiating bandwidth.

Since the isolation is achieved by using a parasitic decoupling structure, therefore there is the possibility of a reduction in radiation efficiency. To further analyse the effect of decoupling structure on radiation characteristics, the antenna efficiency is simulated with and without decoupling structure. The comparison is provided in Fig. 11.

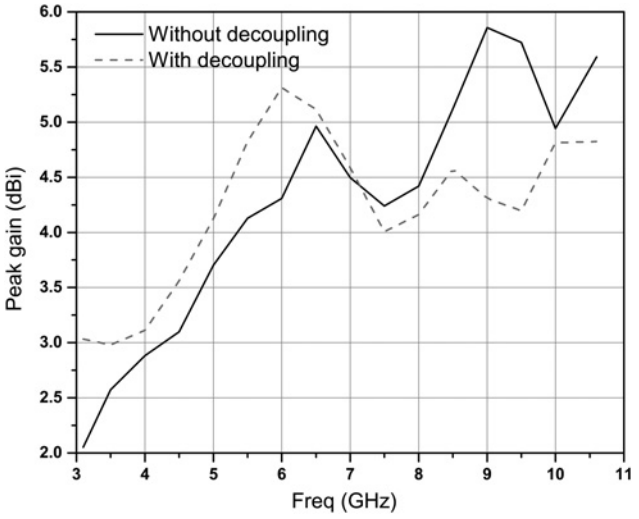

Fig. 10 *Simulated antenna gain variation over the radiating band*

The total efficiency (radiation efficiency taking into account also return loss) of antenna remains above 85% in the complete band. The variation in radiation efficiency as a function of frequency is also plotted to analyse the behaviour of antenna efficiency. The radiation efficiency only varies by <2% in the complete band which certifies that the parasitic decoupling structure does not have any notable effect on radiation characteristics. The total efficiency at the lower UWB frequencies is better for diversity antenna with decoupling structure which indicates that the decoupling structure actually reduces the return loss at lower frequencies. At the upper UWB frequencies, the total efficiency with decoupling structure is less than the antenna without decoupling structure which indicates increase in mismatch loss at higher frequencies.

5 Diversity analysis

Diversity performance of antenna has been investigated by computing correlation coefficient. For isotropic distribution ECC can be approximated by using scattering matrix as proposed by Blanch *et al.* [17]. A comparison of ECC computed from *S* parameters for diversity antennas with and without decoupling structure is shown in Fig. 12*a*.

The ECC computed from *S* parameters is approximated for ideal uniform scattering environment. In order to further investigate the diversity performance, the ECC was numerically computed by using far-field radiation patterns according to (1), [18]. The three-dimensional radiation patterns were simulated using commercially available simulator [16], where XPR is cross-polarisation ratio. P_θ and P_φ are θ and φ components of angular density functions of incoming wave. For indoor and outdoor environments, the angular density functions are considered to be Gaussian in elevation plane and uniform in azimuth plane and they are given by the following

$$\rho_e = \frac{\left|\int_0^{2\pi}\int_0^{\pi}\left(\mathrm{XPR}\,E_{\theta 1}E_{\theta 2}^{*}P_\theta + E_{\varphi 1}E_{\varphi 2}^{*}P_\varphi\right)\mathrm{d}\Omega\right|^2}{\int_0^{2\pi}\int_0^{\pi}\left(\mathrm{XPR}\,E_{\theta 1}E_{\theta 1}^{*}P_\theta + E_{\varphi 1}E_{\varphi 1}^{*}P_\varphi\right)\mathrm{d}\Omega\int_0^{2\pi}\int_0^{\pi}\left(\mathrm{XPR}\,E_{\theta 2}E_{\theta 2}^{*}P_\theta + E_{\varphi 2}E_{\varphi 2}^{*}P_\varphi\right)\mathrm{d}\Omega} \quad (1)$$

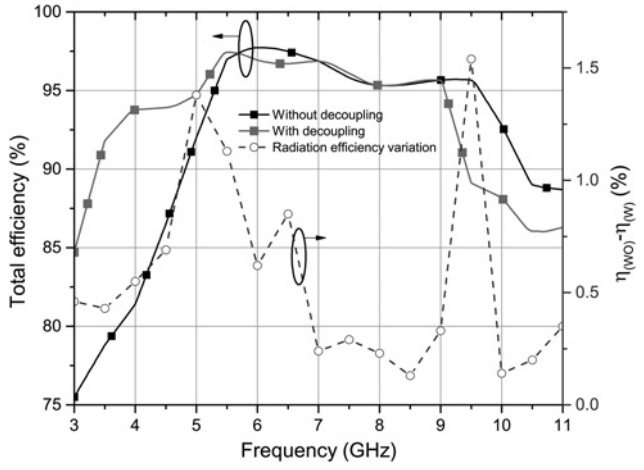

Fig. 11 *Simulated antenna efficiency analysis; total efficiency (left scale) against difference in radiation efficiencies (right scale)*

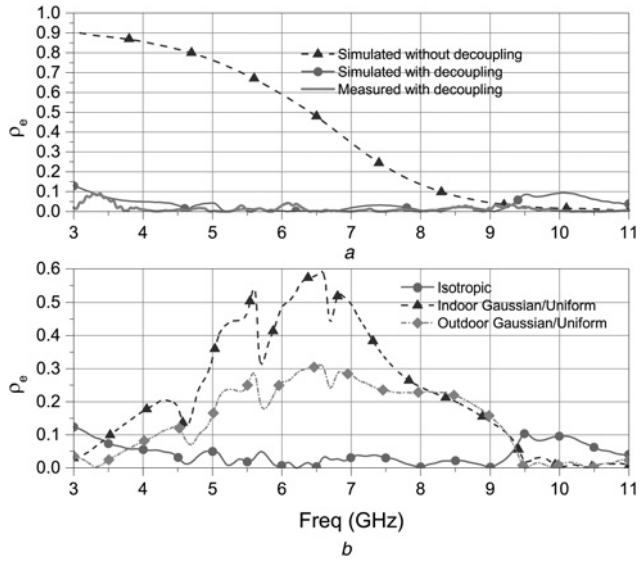

Fig. 12 *Envelope correlation coefficient*

a Simulated and measured ECC using *S* parameters
b Simulated ECC for indoor environment with $m_v = m_H = 10^o$, $\sigma_v = \sigma_H = 15^o$, XPR = 5 dB and for outdoor environment with $m_v = m_H = 20^o$, $\sigma_v = \sigma_H = 30^o$ and XPR = 1 dB

equations [19, 20]

$$P_\theta(\theta,\ \varphi) = A_\theta \exp\left[-\frac{\{\theta - (\pi/2 - m_v)\}^2}{2\sigma_v^2}\right] \times (0 \le \theta \le \pi,\ -\pi \le \varphi \le \pi) \quad (2)$$

$$P_\varphi(\theta,\ \varphi) = A_\varphi \exp\left[-\frac{\{\theta - (\pi/2 - m_H)\}^2}{2\sigma_H^2}\right] \times (0 \le \theta \le \pi, -\pi \le \varphi \le \pi) \quad (3)$$

where constants A_θ and A_φ are considered such that (4) and

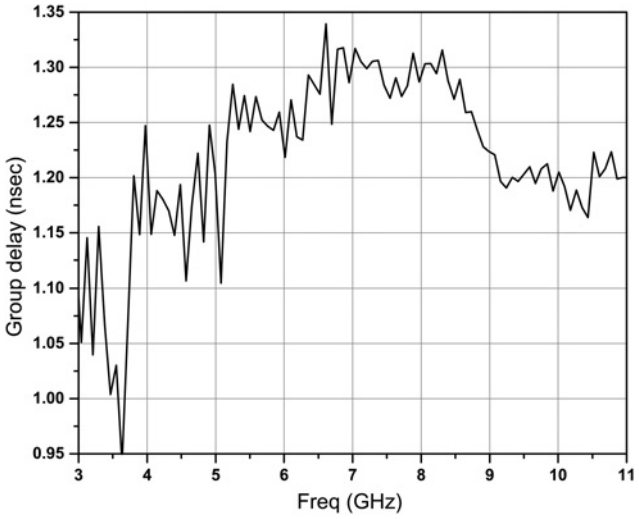

Fig. 13 *Measured group delay as a function of frequency of the proposed UWB diversity antenna*

(5) are justified

$$\int_{-\pi}^{\pi}\int_{0}^{\pi} P_\theta(\theta,\ \varphi)\sin\theta\,d\theta\,d\varphi = 1 \quad (4)$$

$$\int_{-\pi}^{\pi}\int_{0}^{\pi} P_\varphi(\theta,\ \varphi)\sin\theta\,d\theta\,d\varphi = 1 \quad (5)$$

m_v and m_H are mean elevation angle for vertically and horizontally polarised components of incoming wave, respectively, and σ_v and σ_H are their standard deviations. The ECC for isotropic, indoor and outdoor environments for the proposed antenna is shown in Fig. 12*b*. The ECC for isotropic, indoor and outdoor environments are below 0.6 in the complete band ensuring good diversity performance.

Time domain performances of the proposed UWB-MIMO antenna array were also verified by measuring the group delay. A pair of identical antenna arrays was placed face-to-face at a distance of 12 cm with port 1 of both antennas connected to the VNA, whereas port 2 were terminated with a load of 50 Ω. The result is shown in Fig. 13. The group delay variation is <350 ps for the entire UWB spectrum.

6 Conclusion

An UWB diversity antenna with a floating parasitic digitated decoupling structure has been proposed. The detailed analysis on the working of the proposed structure has been provided. The measured reflection coefficient and mutual coupling are better than −10 and −20 dB, respectively, in most of the bandwidths. Peak gain variation is <2.3 dBi and the ECC for isotropic scattering environment is better than 0.09 and for indoor and outdoor environments is better than 0.6 and 0.3, respectively. The fabricated prototype measures 33×45.5 mm^2 only which makes it suitable for handled portable devices, PDAs and next generation home entertainment gadgets.

doi: 10.1049/iet-map.2013.0672

7 References

1 Sibille, A.: 'Time-domain diversity in ultra-wideband MIMO communications', *EURASIP J. Appl. Signal Process.*, **2005**, (3), pp. 316–327
2 Foschini, G.J., Gans, M.: 'On limits of wireless communications in a fading environment when using multiple antennas', *Wirel. Personal Commun.*, 1998, **6**, (3), pp. 311–335
3 Wallace, J., Jensen, M., Swindlehurst, A., Jeffs, B.: 'Experimental characterization of the MIMO wireless channel: data acquisition and analysis', *IEEE Trans. Wirel. Commun.*, 2003, **2**, (2), pp. 335–343
4 Weber, J., Volmer, C., Blau, K., Stephan, R.: 'He in M.A. Miniaturized antenna arrays using decoupling networks with realistic elements', *IEEE Trans. Microw. Theory Tech.*, 2006, **54**, (6), pp. 2733–2740
5 Shanawani, M., Paul, D.L., Dumanli, S., Railton, C.: 'Design of a novel antenna array for MIMO applications'. Proc. Third Int. Conf. Information and Communication Technologies, from Theory to Applications, April 2008
6 Ranvier, S., Luxey, C., Suvikunnas, P., Staraj, R., Vainikainen, P.: 'Mutual coupling reduction for patch antennas array'. Proc. IEEE Int. Symp. Antennas and Propagation Society, June 2007, pp. 3632–3635
7 Chebihi, A., Luxey, C., Diallo, A., Le Thuc, P., Staraj, R.: 'A novel isolation technique for closely spaced PIFAs for UMTS mobile phones', *IEEE Antennas Wirel. Propag. Lett.*, 2008, **7**, pp. 665–668
8 Liu, L., Zhao, H., See, T.S.P., Chen, Z.N.: 'A printed ultra-wideband diversity antenna'. Proc. IEEE Int. Conf. Ultra Wideband, September 2006, vol. 2, pp. 351–356
9 Lin, S.Y., Huang, H.R.: 'Ultra-wideband MIMO antenna with enhanced isolation', *Microw. Opt. Technol. Lett.*, 2009, **51**, (2), pp. 570–573
10 Hong, S., Lee, J., Choi, J.: 'Design of UWB diversity antenna for PDA applications'. Proc. 11th Int. Conf. Advanced Communication Technology, February 2008, pp. 583–585
11 Chen, Y., Lu, W.J., Cheng, C.H., Cao, W., Li, Y.: 'Printed diversity antenna with cross shape stub for ultra-wideband applications'. Proc. 11th IEEE Int. Conf. Communication Systems, November 2008, pp. 813–816
12 Zhang, S., Ying, Z., Xiong, J., Sailing, H.: 'Ultrawide band MIMO/diversity antennas with a tree-like structure to enhance wideband isolation', *IEEE Antennas Wirel. Propag. Lett.*, 2009, **8**, pp. 1279–1282
13 Lau, B.K., Andersen, J.: 'Simple and efficient decoupling of compact arrays with parasitic scatterers', *IEEE Trans. Antennas Propag.*, 2012, **60**, (2), pp. 464–472
14 Min, K.S., Kim, D.J., Moon, Y.M.: 'Improved MIMO antenna by mutual coupling suppression between elements'. European Conf. Wireless Technology, 2005, pp. 125–128
15 Meiguni, J.S., Kamyab, M., Hosseinbeig, A.: 'Effect of parasitic elements in spherical prob-feed antennas'. 21st Iranian Conf. Electrical Engineering (ICEE), May 2013, pp. 1–4
16 CST Microwave Studio Darmstadt, Germany, 2012
17 Blanch, S., Romeu, J., Corbella, I.: 'Exact representation of antenna system diversity performance from input parameter description', *Electron. Lett.*, 2003, **39**, (9), pp. 705–707
18 Taga, T.: 'Indoor measurement method for evaluating statistical distribution of incident waves under out-of-sight condition and experimental studies of characteristics of mobile station polarization diversity', *IEICE Trans.*, 1991, **J74-B-II**, (11), pp. 608–615
19 Ogawa, K., Matsuyoshi, T.: 'An analysis of the performance of a handset diversity antenna influenced by head, hand and shoulder effects at 900 MHz: I – Effective gain characteristics', *IEEE Trans. Veh. Technol.*, 2001, **50**, (3), pp. 830–844
20 Taga, T.: 'Analysis for mean effective gain of mobile antennas in land mobile radio environments', *IEEE Trans. Veh. Technol.*, 1990, **39**, (2), pp. 117–131